Journal of Inclusion Phenomena and Macrocyclic Chemistry (2005) 53:15–22
DOI 10.1007/s10847-004-8212-1

Host–Guest Interactions of Risperidone with Natural and Modified Cyclodextrins: Phase Solubility, Thermodynamics and Molecular Modeling Studies

M.I. El-BARGHOUTHI[1], N.A. MASOUD[1], J.K. Al-KAFAWEIN[1], M.B. ZUGHUL[2,*] and A.A. BADWAN[3]

[1]*Department of Chemistry, The Hashemite University, P.O. Box 150459, Zarqa 13115, Jordan;* [2]*Department of Chemistry, University of Jordan, Amman, Jordan;* [3]*Jordanian Pharmaceutical Manufacturing Company, Naor, Jordan*

(Received 15 June 2004; in final form 27 December 2004)

Key words: binding constants, complex geometries, complexation thermodynamics, cyclodextrins, inclusion complexes, molecular mechanical modeling, risperidone

Abstract

The solubility of risperidone (Risp) in aqueous buffered cyclodextrin (CD) solution was investigated for α-, β-, γ- and HP-β-CD. The effects of pH, ionic strength and temperature on complex stability were also explored. Neutral Risp tends to form higher order complexes (1:2) with both β- and HP-β-CD, but only 1:1 type complexes with α-, and γ-CD. The tendency of Risp to complex with cyclodextrins is in the order β-CD > HP-β-CD > γ-CD > α-CD. The 1:1 complex formation constant of Risp/HP-β-CD increases with increasing ionic strength in an opposite trend to the inherent solubility (S_0) of Risp, thus indicating significant hydrophobic effect. The hydrophobic effect contributes to the extent of 72% towards neutral Risp/HP-β-CD complex stability, while specific interactions contribute only 4.7 kJ/mol. Thermodynamic studies showed that 1:1 Risp/HP-β-CD complex formation is driven by a favorable enthalpy change ($\Delta H^0 = -31.2$ kJ/mol, $\Delta S^0 = -7$ J/mol.K) while the 1:2 complex is largely driven by entropy changes ($\Delta H^0 = -5.0$ kJ/mol, $\Delta S^0 = 42$ J/mol.K). Complex stability was found to vary with pH, with a higher formation constant for neutral Risp. Molecular mechanical computations using MM (atomic charges and bond dipole algorithms) and Amber force fields, which were carried out to explore possible sites of interactions between Risp and CDs and to rationalize complex stoichiometry, produced similar results concerning optimal inclusion complex geometries and stoichiometries.

Introduction

Cyclodextrins (CDs) can form inclusion complexes in aqueous solution with a wide variety of organic compounds. They are well known for their ability to increase aqueous solubility, stability and bioavailability of many lipophilic drugs [1–3]. Several binding forces have been proposed for the inclusion of substrates into CDs including van der Waals forces, hydrophobic effect, hydrogen bonding, macrocycle relaxation and the release of energetic water molecules from the cavity [4, 5].

Recently, there has been considerable interest in the computer modeling of cyclodextrin complexes. Molecular mechanics [6–13] and molecular dynamic simulation of guest–host interactions [14–17] are now being used as tools for understanding the complexation process, particularly the driving forces for complex formation as well as the optimal geometries of the resulting complexes.

Risperidone (Risp) is an antipsychotic agent belonging to a new chemical class, the benzisoxazole derivatives. Risp acts as an antagonist to both D2 and 5-HT2 receptors in the brain [18]. It is poorly soluble in water, thus causing some difficulties in pharmaceutical formulations of the drug. The utilization of cyclodextrins to enhance the solubility of Risp has not yet been reported in the literature.

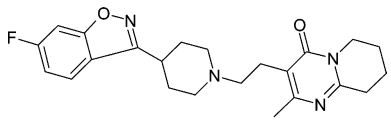

Risp

The present work reports the results of an investigation of the solubility of Risp in aqueous cyclodextrin solutions including those of α-, β-, γ- and HP-β-CDs. The effects of ionic strength, temperature and pH on complex stability in aqueous solutions are also reported. Individual complex formation constants estimated through rigorous analysis of the measured phase solubility diagrams [19–22] are also discussed in terms of the driving forces for complex stability. These were rationalized in terms of thermodynamic analysis combined with molecular mechanics simulations using MM and Amber force fields [23, 24].

* Author for correspondence. E-mail: mbzughul@ju.edu.jo

Experimental

Materials

Risperidone (Risp), α-, β-, γ- and HP-β-CDs were provided by JPM (The Jordanian Pharmaceutical Manufacturing Company, Naor, Jordan). All reagents used were of analytical grade, and doubly distilled deionized water was used throughout.

Instruments

Absorbance measurements were carried out using a Carry 100 Bio spectrophotometer. Optical activity measurements were performed using automatic polarimeter POLAAR 21. DSC curves were recorded on a Mettler TA3000 differential scanning calorimeter at a heating rate of 10 °C/min. A Julabo GLF 1083 thermostatic water bath shaker (±0.2 °C) was used. pH-measurements were carried out using an inoLab pH meter equipped with a combination glass electrode with a stated accuracy of ±0.005 pH units.

Phase solubility studies

Excess amounts of Risp were added to 100 ml screw cap flasks. Solutions of CD of various concentrations were prepared at specific pH values in 0.1 M phosphate buffers. Constant volumes of the cyclodextrin solutions were then added to the flasks. The solutions were shaken in a thermostated water bath for 48 h and then left aside for 24 h to settle and reach equilibrium at fixed temperature. The solutions were then filtered using a 0.45 μm membrane filter. The filtrates were appropriately diluted with the buffer solution of the same pH. The concentration of Risp in each solution was determined by measuring the absorbance at $\lambda_{max} = 238$ nm. For inverted phase solubility diagrams in which the solubility of CD was measured against Risp concentration at low pH, the solutions were treated in the same manner as in normal phase solubility diagrams except that the solutions were diluted with 0.1 M phosphate buffer at pH = 2.0 and analyzed on the polarimeter to measure the solubilty of β-cyclodextrin. pH solubility profiles were also determined in a similar manner.

Preparation of the complex precipitate

The solid complex precipitate was prepared in a 0.1 M phosphate buffer solution at pH = 10.5 using appropriate amounts of the guests and β-CD. The solution was shaken for 48 h at constant temperature. The resulting precipitate was collected by suction filtration, dried under vacuum and analyzed for drug and β-CD content.

Estimation of stability constants

Phase solubility diagrams were analyzed to obtain estimates of the complex formation constants of soluble SL_2 complexes following rigorous procedures described earlier [20–22]:

The solubility (S_{eq}) of Risp in aqueous CD solutions of variable concentrations is given by:

$$\begin{aligned} S_{eq} &= S_0 + [SL] + [SL_2] \\ &= S_0 + K_{11}S_0[L] + K_{11}K_{12}S_0[L]^2 \end{aligned} \quad (1)$$

where S_0 is the solubility at zero CD concentration, S and L denote Risp and CD, respectively, while SL and SL_2 represent the 1:1 and 1:2 type complexes. The total concentration of CD in soln (L_{eq}) is given by

$$\begin{aligned} L_{eq} &= [L] + [SL] + 2[SL_2] \\ &= [L] + K_{11}S_0[L] + 2K_{11}K_{12}S_0[L]^2 \end{aligned} \quad (2)$$

$[L]$ is the concentration of free CD molecules given by

$$[L] = (-b \pm (b - aL_t)^{1/2})/(2a) \quad (3)$$

where $a = 2\ K_{11}\ K_{12}\ S_0$ and $b = 1\ +\ K_{11}\ S_0$, while K_{11} and K_{12} define the individual formation constants of SL and SL_2 complexes, respectively. Non-linear regression of experimental data corresponding to each phase diagram were conducted to obtain S_0, K_{11} and K_{12} by minimizing the sum of squares of errors given by

$$SSQ = \Sigma(S_{eq} - S_{eq}^{p})^2 \quad (4)$$

where S_{eq}^{P} is the predicted equilibrium solubility of Risp given by Equation 1.

Molecular modeling

Computations in vacuum and in water were performed with Hyperchem® (release 6.03 professional, Hypercube Inc., Waterloo, Canada). Force fields used in these computations were Amber and enhanced MM method implemented in Hyperchem® using the atomic charges or bond dipoles options for calculation of electrostatic interactions. Partial atomic charges were obtained by performing AM1 semi-empirical calculations [25]. Energy minimization was performed using the conjugate gradient algorithm (0.01 kcal/mol Å gradient).

The initial molecular geometries of CDs were obtained using X-ray diffraction data [26–29]. These geometries were optimized again using the Amber force field by imposing a restraint on the dihedral angles to the average values [28]. Risp was built up from standard bond lengths and bond angles. The resulting structure was then minimized with the Amber and MM force fields.

Results and discussion

Acid–base ionization constants

The pH solubility profile of Risp in aqueous 0.1 M phosphate buffer solution at 25 °C is shown in

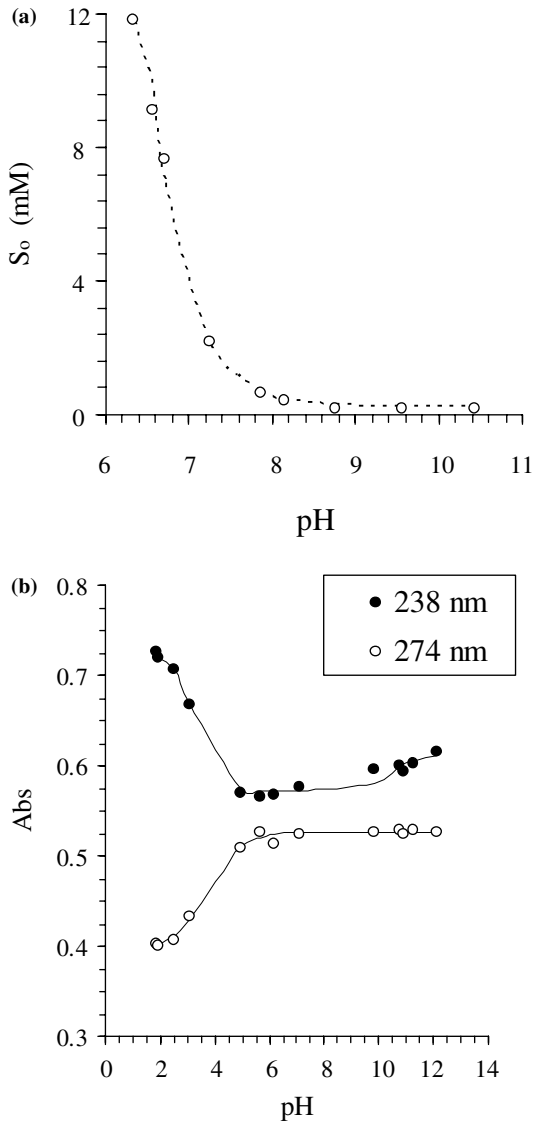

Figure 1. (a) pH solubility profile of Risp and (b) the absorbance of 0.048 mM Risp *versus* pH measured in 0.1 M phosphate buffer solution at 25 °C.

Figure 1a. Non-linear regression of the pH profile yielded a pK_{a1} value of 8.1 for monoprotonated Risp. The dotted line represents the best fit of the experimental data. Attempts to obtain pK_{a2} for Risp from the pH solubility profile were unsuccessful due to difficulties in pH control at low pH. Therefore, the absorbance at 238 and 274 nm of a fixed concentration of Risp (0.048 mM) in 0.1 M phosphate buffer was measured at different pHs at 25 °C which is depicted in Figure 1b. Non-linear regression of the data represented in Figure 1b yielded an estimate of pK_{a2} of 3.1 for diprotonated Risp. The variation of Risp absorbance at pH >5 was relatively small, thus making accurate estimation of pK_{a1} by this method inadequate.

Phase solubility studies

To obtain reasonable estimates of the complex formation constants of Risp with α-, *β*-, *γ*- and HP-*β*-CD, the solubility of Risp was measured against CD concentration in 0.1 M phosphate buffer at high pH where the inherent solubility of Risp (S_0) is lower than that of the CD. At lower pH (<6) where S_0 of Risp exceeds that of *β*-CD, inverted phase solubility diagrams were established by measuring the solubility of *β*-CD against Risp concentration.

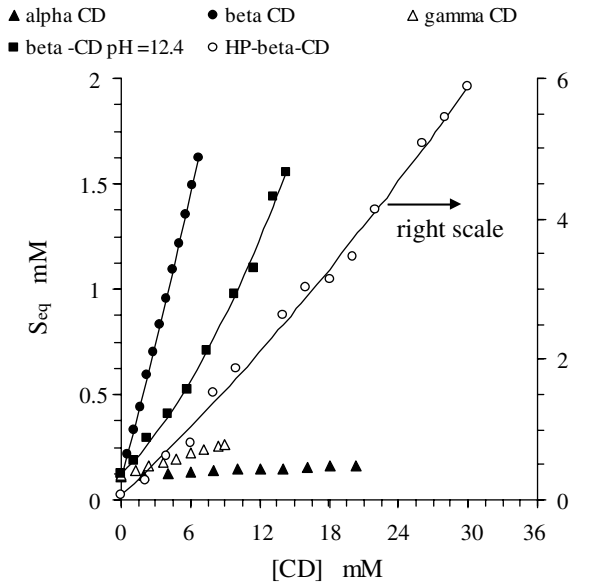

Figure 2. Phase solubility diagram of Risp against α-, *β*-, *γ*- and HP-*β*-CDs obtained in 0.1 M phosphate buffer and 25 °C at pHs = 10.5 and 12.4.

Figure 2 depicts phase solubility diagrams (PSDs) obtained for Risp against each of α-, *β*-, *γ*- and HP-*β*-CD concentration at pH 10.5 and 25 °C. At this pH, Risp exists as a neutral molecule (p$K_{a1} = 8.1$) with an inherent solubility (S_0) of 0.109 mM. Rigorous analysis [20–22] of the PSDs yielded complex stoichiometries and estimates of complex formation constants that are listed in Table 1. It was observed that both *β*-CD and HP-*β*-CD form 1:1 and 1:2 soluble complexes with K_{11} and K_{12} values of 2472 and 53 M^{-1} for *β*-CD, and 2257 and 22 M^{-1} for HP-*β*-CD. It was also observed that the 1:2 Risp/*β*-CD complex reaches saturation at 7 mM *β*-CD while that of HP-*β*-CD remains soluble, which is apparently due to the much

Table 1. Estimates of complex formation constants for Risp/α-, *β*-, *γ*- and HP-*β*-CDs obtained from non-linear regression of PSDs in 0.1 M phosphate buffer at 25 °C

Host	PH	K_{11} (M^{-1})	K_{12} (M^{-1})
α-CD	10.50	24	–
β-CD	2.00[a]	112	–
	5.62[a]	943	–
	10.50	2472	53
	12.40	432	101
γ-CD	10.50	143	–
HP-*β*-CD	10.50	2257	22

[a] Inverted phase solubility diagram.

higher inherent solubility of HP-β-CD in water. The complex formation constants (K_{11} and K_{12}) are also slightly higher for β-CD than HP-β-CD, probably for the same reason (hydrophobic effect). It is interesting to note that earlier studies indicated that the hydroxypropyl groups in HP-β-CD may facilitate inclusion [30] or hinder inclusion of bulky substrates [31–33]. In contrast, both α- and γ-CDs form only 1:1 type complexes with much lower K_{11} values (24 M^{-1} for α-CD and 143 M^{-1} for γ-CD). This is most likely due to two factors: (a) both α- and γ-CD are more soluble in water than β-CD thus lowering the driving force to complex with Risp, and (b) α-CD has a small cavity size that reduces the probability of including either of the two peripheral bulky groups of Risp, while γ-CD has a larger cavity size than β-CD thus lowering effective interactions with Risp. It was also interesting to observe that the 1:1 Risp/γ-CD complex reaches saturation at 10 mM γ-CD concentration beyond which the complex precipitates. Earlier studies indicated that γ-CD tends to form less stable complexes due to its relatively larger cavity size, which prohibits an effective geometric fit [31]. This, combined with the fact that γ-CD is more soluble in water, is certainly responsible for the lower K_{11} value observed for Risp/γ-CD (143 M^{-1}) than those of Risp/β-CD (2472 M^{-1}) and Risp/HP-β-CD (2257 M^{-1}); the latter two CDs having appropriate cavity sizes that interact more favorably with Risp.

Quantification of the hydrophobic effect

To find out how a change in the inherent solubility (S_0) of either Risp or CD may affect complex stability in solution, two more types of PSDs were measured. First, the solubility of Risp was measured against β-CD concentration at pH 12.4, where β-CD becomes more soluble due to partial ionization of the β-CD hydroxyl groups (pK_a = 12.1). This is shown in Figure 2 where the PSD is clearly of A_P type and both 1:1 and 1:2 soluble complexes are formed with K_{11} = 432 M^{-1} and K_{12} = 101 M^{-1}. Obviously, the driving force for 1:1 complex formation is lower at pH 12.4 where β-CD is more soluble than at pH = 10.5. This is in line with earlier studies suggesting that charged CDs are less likely to form complexes due to a corresponding lower tendency for desolvation [34, 35]. The fact that K_{12} is larger (101 M^{-1}) at pH 12.4 than at 10.5 (53 M^{-1}) for Risp/β-CD is most likely due to enhanced hydrogen bonding interactions with two partially ionized β-CD molecules enclosing Risp at pH 12.4.

To explore this further, two other PSDs were obtained by measuring the solubility of β-CD against Risp concentration (Inverted PSDs) at pH = 5.6 and 2.0, where the solubility of Risp exceeds that of β-CD (16 mM at 25 °C). These are depicted in Figure 3, which subscribe to 1:1 type soluble complexes as was determined through rigorous analysis. The corresponding K_{11} values were 943 M^{-1} at pH = 5.6 where the solubility of Risp exceeds 36 mM, and 112 M^{-1} at pH = 2.0 where

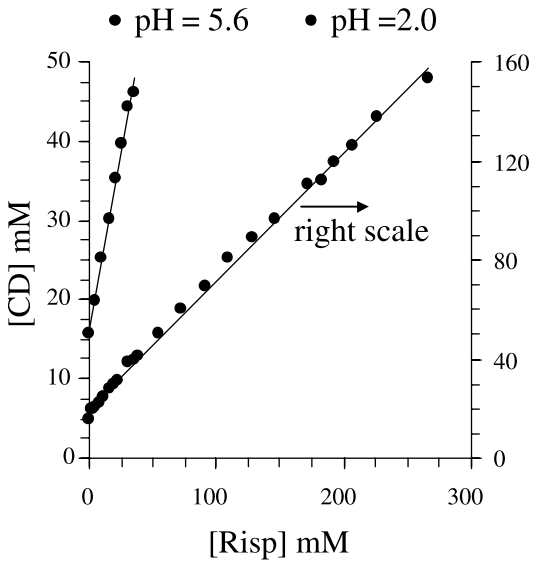

Figure 3. Inverted phase solubility diagrams of β-CD against Risp in 0.1 M phosphate buffer and 25 °C obtained at pHs = 2.0 and 5.6.

the solubility of Risp exceeds 250 mM (Table 1). Thus it is evident that soluble complex stability decreases as the inherent solubility (S_0) of either Risp or β-CD increases. This certainly indicates that the hydrophobic effect does have a significant contribution towards soluble complex stability.

To have a quantitative estimate of the contribution of the hydrophobic effect to complex stability in comparison with other factors such as specific interactions, two procedures were attempted. One was to obtain estimates of K_{11} from PSDs measured at different pHs where S_0 varies for Risp, then plot $-RT \ln K_{11}$ against $-RT \ln S_0$. Unfortunately, this route could not be followed with sufficient precision due to the rather high solubility of Risp at low pH where pH control becomes impossible. The second route followed was to measure the PSDs at same pH but different ionic strengths where S_0 for Risp decreases with increasing ionic strength. The results are listed in Table 2 for neutral Risp/HP-β-CD and the corresponding plot of $-RT \ln K_{11}$* against $-RT \ln S_0$* (the asterisk indicates the mole fraction standard state) is depicted in Figure 4. From the slope (-0.717), it is clear that the hydrophobic effect contributes to the extent of 72% towards neutral complex stability, while specific interactions contribute only about 4.7 kJ/mol (intercept).

Table 2. Estimates of complex formation constants obtained from non-linear regression of PSDs for Risp/HP-β-CD at different ionic strengths in phosphate buffer at pH 10.5 and 25 °C

Ionic strength (M)	0.14	0.33	0.44	0.60	0.92	1.21
S_0 (mM)	0.160	0.140	0.121	0.095	0.074	0.034
K_{11} (M^{-1})	1031	1320	1288	1549	1740	3373

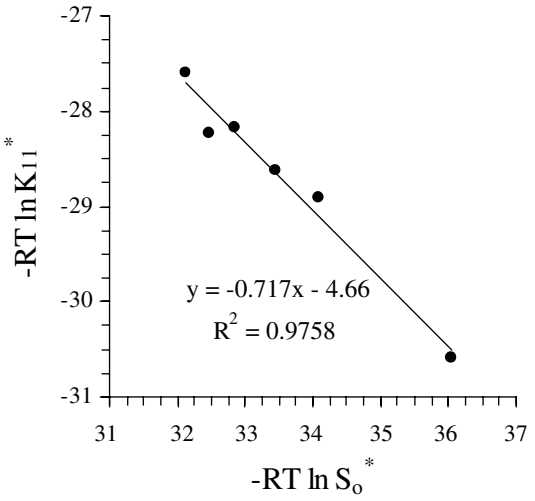

Figure 4. Plot of $-RT\ln K_{11}^*$ against $-RT\ln S_0^*$ for Risp/HP-β-CD complexation in different concentrations of phosphate buffer at 30 °C and pH = 10.4.

Thermodynamics

The effect of temperature on complex stability was studied by measuring PSDs for the neutral Risp/HPβ-CD system at pH = 10.5 and different temperatures (25–50 °C). Figure 5 shows van't Hoff plots of ln K_{11}^* and ln β_{12}^* against 1/T, while Table 3 lists the corresponding thermodynamic parameters ($\beta_{12} = K_{11}K_{12}$). It is observed that 1:1 complex formation with HP-β-CD is largely driven by favorable enthalpy change (−31.2 kJ/mol) but is slightly hindered by an unfavorable entropy change ($\Delta S^0 = -7$ J/mol K). In contrast, 1:2 complex formation is driven by a slight enthalpy change ($\Delta H^0 = -5.0$ kJ/mol) but more significant entropy change ($\Delta S^0 = 42$ J/mol K). This indicates that the 1:1 complex is more tightly bound with a consequent restricted structure, while 1:2 complex formation is accompanied by more desolvation of Risp and hence an appreciable favorable entropy change.

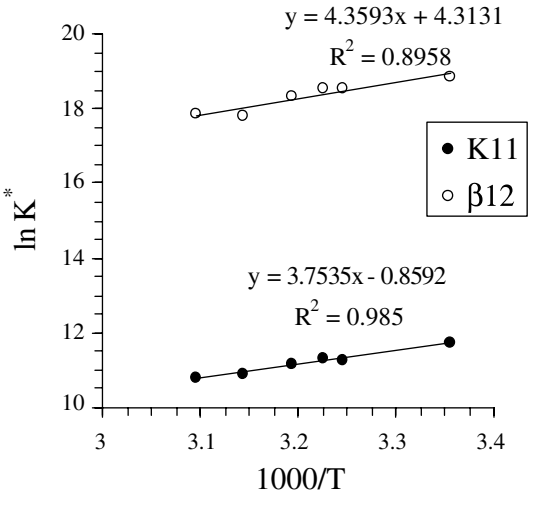

Figure 5. Plot of ln K_{11}^* and ln β_{12}^* against 1000/T (K^{-1}) of the Risp/HP-β-CD system in 0.1 M phosphate buffer at pH = 10.5.

Table 3. Thermodynamic parameters of Risp/HP-β-CD complex obtained in 0.1 M phosphate buffer at pH 10.5 and 25 °C (numbers in brackets indicate error limits for a 95% confidence level)

Equilibrium reaction; Equilibrium constant	ΔG^0 (kJ/mol)[a]	ΔH^0 (kJ/mol)[a]	ΔS^0 (J/mol K)
$S_{(aq)} + L_{(aq)} \leftrightarrows SL_{(aq)}; K_{11}$	−29.1 (2.7)	−31.2 (1.9)	−7 (3)
$SL_{(aq)} + L_{(aq)} \leftrightarrows SL_{2(aq)}; K_{12}$	−17.8 (4.1)	−5.0 (3.0)	42 (6)
$S_{(aq)} + 2L_{(aq)} \leftrightarrows SL_{2(aq)}; \beta_{12}$	−46.9 (6.8)	−36.2 (4.9)	35 (6)

[a]Mole fraction standard state.

Risp/β-CD solid complex stoichiometry

Chemical analysis of the neutral Risp/β-CD complex precipitate, which was obtained at pH 10.5, indicated 1:2 stoichiometry. The solid complex stoichiometry was determined by measuring the number of moles of Risp (spectrophotometrically) and β-CD (polarimetrically) of pre-weighed samples of the isolated and dried solid complex. The samples were dissolved into appropriate volumes of 0.1 M phosphate buffer at the same pH corresponding to those of Risp absorbance and β-CD optical rotation calibration curves.

DSC thermograms of Risp, β-CD, a 1:2 physical mixture of Risp with β-CD and the solid 1:2 complex obtained at pH = 10.5 are shown in Figure 6. Risp exhibits an endothermic peak at 172 °C corresponding to its melting point, which also appears in the physical mixture but disappears completely in the DSC thermogram of the 1:2 solid complex. This clearly indicates the formation of an inclusion and not a peripheral complex.

Molecular modeling

The coordinate system used to define the process of complexation is shown below for the two possible approaches A and B. Initially, the position of the CD macrocycle was fixed while the guest approaches along the x-axis toward the wider rim of the CD cavity (two

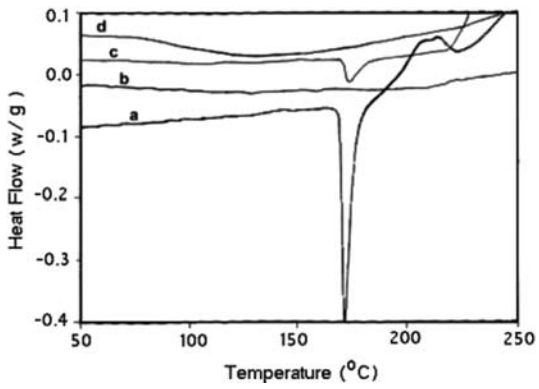

Figure 6. DSC thermograms for (a) Risp, (b) β-CD, (c) a 1:2 physical mixture of Risp and β-CD and (d) the 1:2 Risp/β-CD complex.

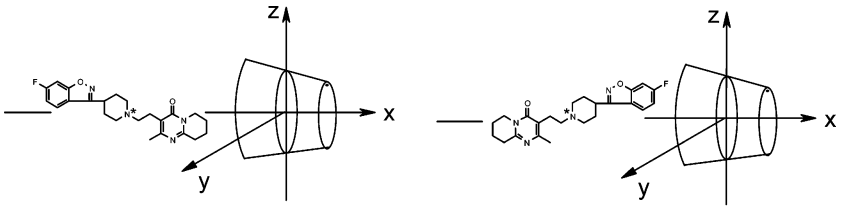

Approach A Approach B

orientations were taken). The central atom was defined in the guest molecule near the center of mass. It was set initially at an x-coordinate of −20 Å and was moved through the CD wider cavity along the x-axis to +20 Å in 1 Å steps. The structures generated at each step were optimized from the initial conformations, while keeping the CD structure fixed. The structures obtained at the minima of the energy surface were then minimized without restriction to either Risp or CD at 0.01 kcal/mol/Å gradient.

The binding energy, E_{binding}, was obtained as the energy of the complex minus the sum of individual Risp and CD energies according to [8–10]:

$$E_{\text{binding}} = E_{\text{guest/CD}} - (E_{\text{isolated guest}} + E_{\text{isolated CD}})$$

For 1:2 complexation, a second CD molecule was introduced manually to the already optimized 1:1 complex in different possible orientations. The substrate was optimized alone first and then the resulting complex was optimized free of any restrictions at 0.01 kcal/mol/Å gradient.

The binding energy (E_{binding}) obtained in vacuum was plotted against the x-coordinate for approaches A and B using $MM_{\text{bond dipole}}$, $MM_{\text{atomic charges}}$ and Amber force fields. As an example, the corresponding plots of the 1:1 Risp/β-CD complex system are depicted in Figure 7, which indicates that the three algorithms yield almost the same energy minima but different E_{binding} values. In each case, three distinct minima are evident for each approach (A and B), which are almost mirror images to each other.

The whole system at the minimum with the lowest energy for either approach was placed in a water box of periodic boundary conditions at same dimensions, and was left to interact free of restrictions to either Risp or CD and $E_{\text{guest/CD}}$ was computed. The same procedure was repeated for individual Risp and CD molecules optimized in the water box to obtain $E_{\text{isolated guest}}$ and $E_{\text{isolated CD}}$ in water, respectively. The corresponding E_{binding} values obtained for Risp/β-CD and Risp/γ-CD in water are listed in Table 4 for both A and B approaches.

Aside from the $MM_{\text{bond dipols}}$ force field predicting approach A to yield a slightly more favorable geometry for the 1:1 Risp/β-CD complex (error limit on E_{binding} values is ±0.4 kcal/mol), approach B appears to be the more favorable route of interaction leading to a more stable Risp/β-CD complex geometry in the

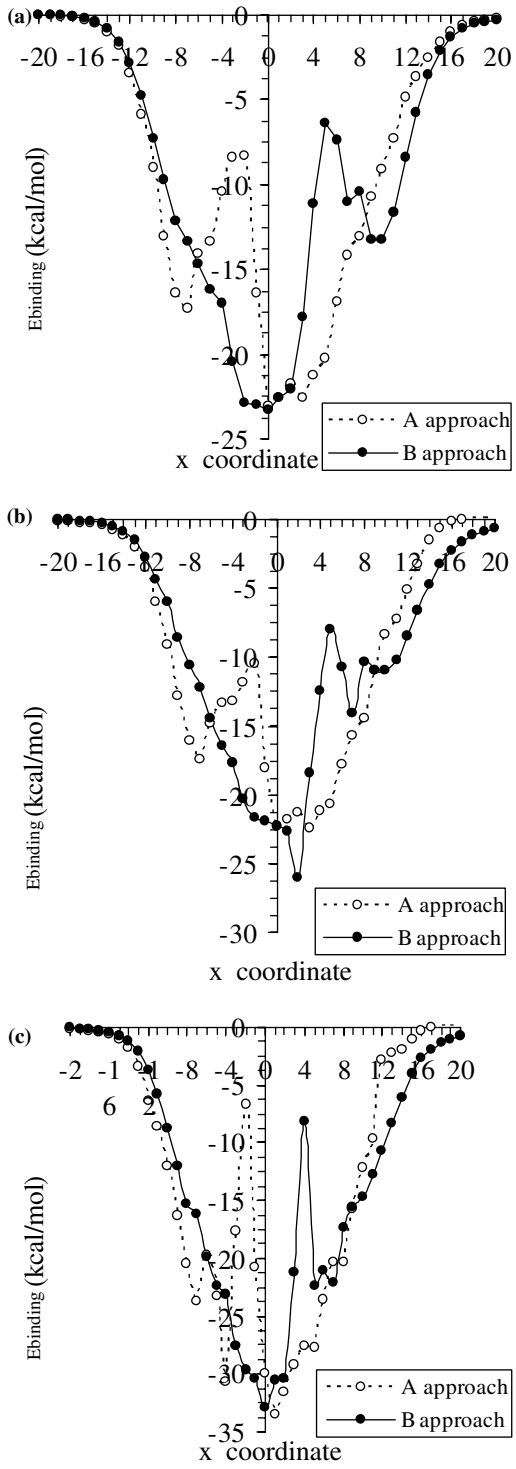

Figure 7. The Risp/β-CD binding energy (E_{binding}) in vacuum plotted against the x-coordinate for approaches A and B using (a) $MM_{\text{bond dipole}}$, (b) $MM_{\text{atomic charges}}$ and (c) Amber force fields.

Table 4. $E_{binding}$ (kcal/mol) of optimal Risp:CD complex geometries obtained following removal of all restrictions on Risp and CD interactions in water (error limit on Ebindinf value is ±0.4 kcal/mol)

	Approach	$MM_{bond\ dipoles}$	$MM_{atomic\ charges}$	Amber
β-CD	A	−20.2	−27.6	−27.5
	B	−19.3	−31.4	−31.6
γ-CD	A	−15.2	−13.2	−36.3
	B	−9.9	−10.3	−34.5

$MM_{atomic\ charges}$ and Amber force fields. In contrast, approach A is predicted to be more favorable for Risp/γ-CD complexation by all three force fields. The fact that the three force fields predict different $E_{binding}$ values, for the same system and same approach, is due to the use of different model compounds in the parameterization procedures of these force fields [23, 24]. Therefore, $E_{binding}$ values can be used to indicate which complex geometry is more favorable but no more quantitative significance be attached to the absolute values, especially when comparing $E_{binding}$ values obtained from different force fields. Nevertheless, it seems better to inspect the results obtained from different force fields in order to come out with a more educated prediction of optimal complex geometries. This is obviously true since the optimal complex geometries predicted by the three force fields were approximately the same, even though the corresponding $E_{binding}$ estimates were different in magnitude.

Figure 8 depicts side views of the optimal 1:1 complex configurations obtained for neutral Risp with α-CD, γ-CD and β-CD. For Risp/α-CD, only partial inclusion takes place thus confirming the low tendency of α-CD to complex obtained from phase solubility analysis ($K_{11} = 24\ M^{-1}$, Table 1). In contrast, optimal interactions involve a complete penetration of the piperidine group of Risp into the cavity of both γ-CD and β-CD, leaving the two peripheral groups protruding outside.

In the 1:1 Risp/β-CD complex, the tetrahydro pyrido group and the pyrido and pyrimidin-4-one nitrogen atoms appear completely protruding outside of the wide cavity rim leaving the carbonyl group to interact more favorably through hydrogen bonding with the secondary hydroxyl group network. The β-CD macrocycle is not distorted and seems to enclose the piperidine group in a configuration that is centrally symmetric to the cavity thus affecting a tighter fit than is observed for the larger γ-CD. A tighter Risp/β-CD cavity fit appears to explain the large enthalpy change ($\Delta H^0 = -31.2$ kJ/mol) and negative entropy change ($\Delta S^0 = -7$ J/mol K) observed for 1:1 complex formation (Table 3), which results from enthalpy-entropy compensation. Figure 8 also shows the optimal 1:2 Risp/β-CD complex configuration, which was only arrived at by having the second β-CD molecule approach through its wide rim, across the tetrahydro pyrido group, towards the wide rim of the first β-CD in the 1:1 complex. In this configuration, the secondary hydroxyl group networks of both β-CDs lie opposite to each other to interact through hydrogen bonding with very little distortion in either macrocycle. This complete enclosure of Risp by the two β-CD molecules appears to enhance desolvation, which is responsible for the positive entropy change ($\Delta S^0 = 42$ J/mol.K) observed for 1:2 complex formation (Table 3).

Conclusion

Neutral Risp tends to form higher order complexes (1:2) with β- and HP-β-CDs but only 1:1 complexes with α- and γ-CDs. Protonated Risp forms only 1:1 complexes with β-CD having lower complex formation constants

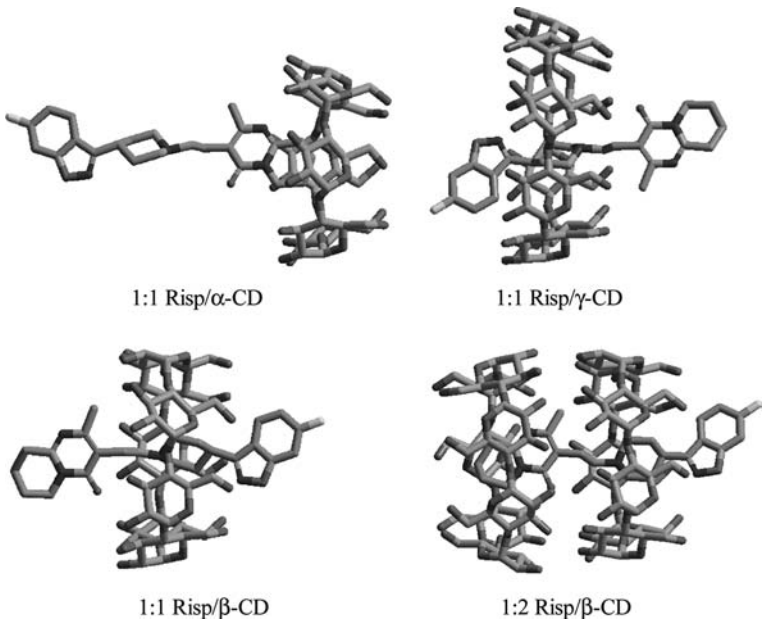

Figure 8. Side views of optimal complex configurations obtained in water using $MM_{bond\ dipoles}$ force field for 1:1 Risp complex with α-CD, γ-CD and β-CD, and the 1:2 Risp: β-CD complex.

(lower K_{11}). This agrees with the fact that K_{11} increases with an increase in pH up to pH 12. Beyond pH 12, CD begins to ionize thus becoming more soluble and K_{11} decreases due to a lower driving force for 1:1 complexation. In contrast, K_{12} increases due to more favorable hydrogen bonding interactions between partially ionized β-CD molecules enclosing the drug substrate. The hydrophobic effect appears to contribute about 72% towards neutral complex stability, while specific interactions contribute only 4.7 kJ/mol. Thermodynamic parameters for Risp/HP-β-CD show that 1:1 complex is driven by enthalpy but retarded by entropy changes. In contrast, 1:2 complex formation is largely favored by entropy but slight enthalpy changes, which are due to higher desolvation induced by total enclosure of Risp with two favorably interacting CD molecules. Molecular mechanical modeling, using MM (bond dipoles and atomic charges) and Amber force fields, yield similar optimal complex geometries. They also predict complex stoichiometries that corroborate thermodynamic results, and indicate that van der Waals interactions constitute the major driving force for complexation, with very little contribution from electrostatic forces.

Acknowledgment

The authors wish to thank the Hashemite University for their financial support.

References

1. D. Duchene: *Cyclodextrins and Their Industrial Uses,* Editions de Sante', Paris (1987).
2. J. Szejtli: *Chem. Rev.* **98**, 1743 (1998).
3. K. Uekama, F. Hirayama, and T. Irie: *Chem. Rev.* **98**, 2045 (1998).
4. I. Tabushi, Y. Kiyousuke, T. Sugimoto, and K. Yamamura: *J. Am. Chem. Soc.* **100**, 916 (1978).
5. M.V. Rekharsky and Y. Inoue: *Chem. Rev.* **98**, 1875 (1998).
6. D.J. Barbirica, R.H. de Rossib, and E.A. Castro: *J. Mol. Struct.* (*THEOCHEM*), **537**, 235 (2001).
7. M. Fathallah, F. Fotiadu, and C. Jaime: *J. Org. Chem.* **59**, 1288 (1994).
8. J.M. Madrid, J. Pozuelo, F. Mendicuti, and W.L. Mattice: *J. Coll. Interface. Sci.* **193**, 112 (1997).
9. J.M. Madrid, F. Mendicuti, and W.L. Mattice: *J. Phys. Chem. B*, **102**, 2037 (1998).
10. J.M. Madrid, M. Villafruela, R. Serrano, and F. Mendicuti: *J. Phys. Chem. B*, **103**, 4847 (1999).
11. P.M. Ivanov and C. Jaime: *J. Mol. Struct.* **377**, 137 (1996).
12. E. Cervello and C. Jaime: *J. Mol. Struct. (THEOCHEM)*, **428**, 195 (1998).
13. P. Jiang, H.W. Sun, R.X. Shen, J. Shi, and C.M. Lai: *J. Mol. Struct.* (*THEOCHEM*), **528**, 211 (2000).
14. A. Mele, G. Raffaini, F. Ganazzoli, M. Juza, and V. Schurig: *Carbohydr. Res.* **338**, 625 (2003).
15. M. Faucci, F. Melani, and P. Mura: *Chem. Phy. Lett.* **358**, 383 (2002).
16. F. Melani, N. Mulinacci, A. Romani, G. Mazzi, and F.F. Vincieri: *Int. J. Pharm.* **166**, 145 (1998).
17. E. Cervello, F. Mazzucchi, and C. Jaime: *J. Mol. Struct. (THEOCHEM)*, **530**, 155 (2000).
18. A. Megens: *Psychopharmacol. Berl.* **114**, 9 (1994).
19. T. Higuchi and K.A.Connors: *Phase Solubility Techniques. Adv Anal, Chem. Instrum.* **4**, 117 (1965).
20. M.B. Zughul and A.A. Badwan: *J. Inclu. Phenom. Mol. Recog. Chem.* **31**, 243 (1998).
21. M.B. Zughul, M. Al-Omari, and A.A. Badwan: *Pharm. Dev. Technol.* **3**, 43 (1998).
22. M.B. Zughul and A.A. Badwan: *Int. J. Pharm.* **151**, 109 (1997).
23. N.L. Allinger, Y.H. Yuh, and J.H. Lii: *J. Am. Chem. Soc.* **111**: 8551 (1989).
24. W.D. Cornell, P. Cieplak, C.I. Bayly, I.R. Gould, K.M. Merz, Jr., D.M. Ferguson, D.C. Spellmeyer, T. Fox, J.W. Caldwell, and P.A. Kollman: *J. Am. Chem. Soc.* **117**, 5179 (1995).
25. M.J.S. Dewar, E.G. Zoebisch, E.F. Healy, and J.J.P. Stewart: *J. Am. Chem. Soc.* **107**, 3902 (1985).
26. R. Puliti, C.A. Mattia, and L. Padiano: *Carbohydr. Res.* **310**, 1 (1998).
27. K. Linder and W. Saenger: *Carbohydr. Res.* **99**, 103 (1982).
28. W. Saenger, J. Jacob, K. Gessler, T. Steiner, D. Hoffman, H. Sanbe, K. Koizumi, S.M. Smith and T. Takaha: *Chem. Rev.* **98**, 1787 (1998).
29. K. Harata: *Bull. Chem. Jpn.* **60**, 2763 (1987).
30. A. Yoshida, M. Yamamoto, T. Itoh, T. Irie, F. Hirayama, and K. Uekama: *Chem. Pharm. Bull. Tokyo.* **38**, 176 (1990).
31. F. Kopecky, B. Kopecky, and P. Kaclik: *J. Incl. Phenom.* **39**, 215 (2001).
32. A. Buvari-Barcza and L. Barcza: *Talanta* **49**, 577 (1999).
33. A. Buvari-Barcza, E. Rak, A. Meszaros, and L. Barcza: *J. Incl. Phenom.* **32**, 453 (1998).
34. F. D'Anna, P.L. Meo, S. Riela, M. Gruttadauria, and R. Noto: *Tetrahedron* **57**, 6823 (2001).
35. S.E. Brown, J.H. Coates, P.A. Duckworth, S.F. Lincoln, C.J. Easton, and B.L. May: *J. Chem. Soc., Faraday Trans.* **89**, 1035 (1993).